

## Distribution mechanism of dominant genera and species of bacteria under different river velocity

Weirong Li <sup>1</sup>, Kai Shen <sup>2, a</sup>, Yanfang Li <sup>1</sup>, Dong Pang <sup>1</sup>, Fangfei Liu <sup>1</sup>,  
Huimin Zhou <sup>3</sup>, Lingfei Kong <sup>3</sup>, Xuqiang Huang <sup>3</sup>, Di Tie <sup>2, b</sup>

<sup>1</sup> Dongguan Eontec Co., Ltd, Guangdong 523000, China;

<sup>2</sup> Engineering Research Center of Continuous Extrusion, Ministry of Education, Dalian Jiaotong University, Dalian 116028, China;

<sup>3</sup> School of Materials Science and Engineering, Northeastern University, Shenyang 110819, China.

<sup>a</sup> skpb\_1995@163.com, <sup>b</sup> tie-di@hotmail.com

**Abstract.** Flow velocity as the basic hydrodynamic condition significantly affects bacterial proliferation and biofilm formation, yet how different flow velocity influences the attachment and distribution of dominant bacteria in different ecological types is poorly understood. In this work, We collected samples from the bottom, side walls and water samples at the flow rates of 0.794m/s and 0.538m/s, respectively. Through high-throughput sequencing identification and analysis technology, it was found that the composition abundance of *Acinetobacter* and *Psychrobacter*, as dominant bacteria, could reach 70%-80% in the floating state, and the attached bacteria at low flow rates were about 20% higher than those at high flow rates. The results showed that the high flow rate inhibited the attachment behavior of dominant bacteria and changed the species composition structure in the overlapping area of multiple samples, which provided a new direction for the prevention and control of microbial corrosion and pollution in waters.

**Keywords:**flow velocity; bacterial proliferation; biofilm formation; high-throughput sequencing; dominant bacteria; corrosion and pollution.

### 1. Introduction

Microbiologically influenced corrosion (MIC) or microbial corrosion refers to corrosion affected by the presence of microorganisms, which leads to the deterioration of materials such as iron, steel, concrete and stone [1–4]. Bacteria attach to form biofilm on material surfaces is considered to be a crucial step to initiate microbial corrosion [5], and this process is mainly controlled by the properties of substrata, velocity, light, temperature, and the availability of nutrients [6]. Among them, the flow rate can not only affect the bacterial proliferation, but also change the community structure of biofilm, which has been widely studied [7-10]. However, how the flow rate affects the attachment and distribution of dominant bacteria in different ecological types remains unclear. Here, we divide the water area into high velocity area and low velocity area through measurement, and collect water samples, water bottom samples and structure surface samples to test the quality of DNA extraction and PCR amplification, which met the requirements of high-throughput sequencing for database construction and sequencing. We obtained high-quality sequences and effective sequences through DADA2 denoising and drew Shannon sparse curves of each sample to prove the rationality of sequencing depth. Finally, we carried out high-throughput sequencing identification and analysis and found high flow rate inhibited the attachment behavior of dominant bacteria and changed the species composition structure in the overlapping area of multiple samples, which provided a new direction for the prevention and control of microbial corrosion and pollution in waters.

## 2. Measurement of water parameters and sample collection

### 2.1 Differential Flow Measurements and Sampling Site Selection

In this paper, the velocity of the river water was measured by the buoy velocity measurement method, using 100mm\*100mm\*10mm plastic foam as a buoy, setting the distance interval of 10m, and taking the average value of several tests to obtain the average velocity of the middle of the watershed and the edge of the watershed as 0.794m/s and 0.538m/s, respectively, which was divided into the high velocity zone and the low velocity zone. To investigate the differences in the distribution of benthic, planktonic, and adherent ecological types of the dominant bacterial genera in the waters at different flow velocities, the sampling site is set as river bottom (Fig.1A), water sample, abutment surface (Fig.1B) or inner wall of riverbank (Fig.1C).

### 2.2 Sample collection and pre-processing

After determining the sampling location, samples were collected and categorized as shown in Fig.1. Benthic and attached organisms samples were collected using sterile cotton swabs, placed in sampling bottles (Fig.1D) containing sterile saline and brought back to the laboratory to be shaken until the sample was dislodged from the surface of the swabs, the swabs were removed, and the sample liquid was allowed to settle, the supernatant was removed, and the samples were stored at -80°C and numbered. The planktonic samples were collected directly in sampling bottles with a water volume of about 2L, fixed with a Rugo type solution of the volume of water samples, allowed to settle, removed the supernatant, and the samples were loaded into 10 ml sampling bottles and stored at -80 °C for spare use.

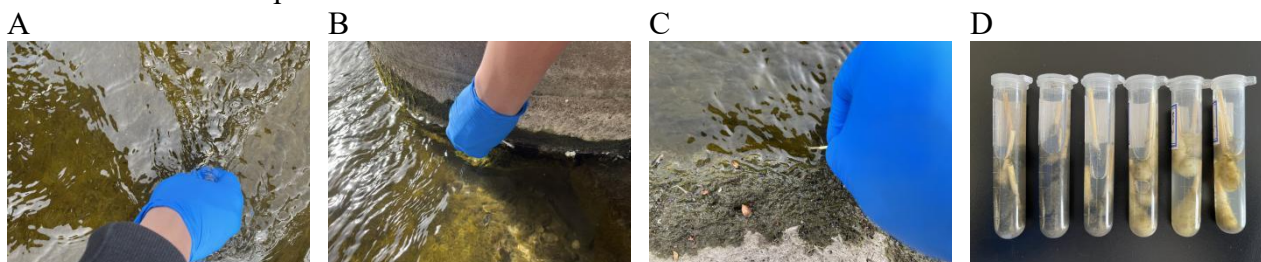


Fig. 1 Diagram of the sample collection site.

## 3. Sample Sequencing and Quality Testing

### 3.1 High-throughput sequencing pre-processing

In this paper, high-throughput sequencing technique was used to identify the species abundance of the collected samples. First, the total DNA of each sample was extracted, and the quality of DNA extraction was detected by 1.2% agarose gel electrophoresis (Fig.2A), and the target sequence of microbial ribosomal RNA or specific gene fragment was used as the target for PCR amplification. Then, the amplified product was purified and recovered by magnetic beads (Fig.2B). The results showed that the quality of DNA extraction was qualified, the experiment was not interfered by external conditions, and the concentration of PCR amplification products met the requirements of sequencing library construction

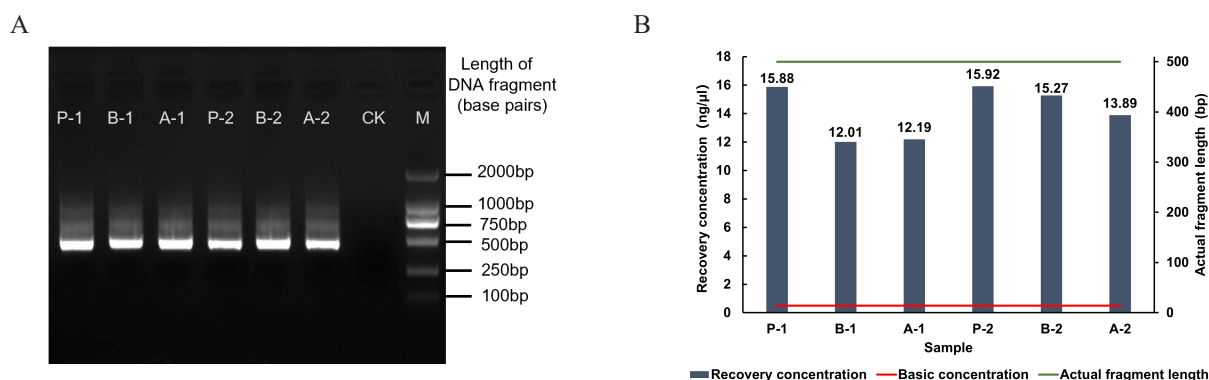


Fig. 2 Results of high-throughput sequencing pre-treatment.

### 3.2 DADA2 denoising to obtain high quality sequences

Quality control, denoising, splicing and de-mosaic analysis were performed on each library by using analysis software QIIME2, and the ASV feature sequence and ASV table were merged, and the sequencing amount of each sample was counted. The results are shown in Table1. P, B and A in SampleID in the table represent the three ecological types of bacteria in the waters, namely planktonic, benthic, and adherent, and 1 and 2 represent the high-flow and low-flow zones, respectively, and the following charts and tables are annotated according to this categorization. In the table, non-chimeric sequences are high-quality sequences; non-singleton is the valid sequence after removing the singleton for the next study.

Table 1 Statistics of sequencing volume per sample

SampleID	Input	Filtered	Denoisied	Merged	Non-chimeric	Non-singleton
P 1	141193	116688	113895	99524	57195	56656
P 2	144849	120390	117018	100151	53244	52546
B 1	135875	113571	109928	86581	52046	51086
B 2	144558	119620	114883	87182	66295	65065
A 1	135561	112227	107226	82587	62918	61831
A 2	145723	122016	117907	94276	59886	58906

### 3.3 Sample sequencing quality analysis

In order to investigate the trend of sample  $\alpha$  diversity with sampling depth, this paper plotted the Shannon [11] sparse curves shown in Fig.3, the flatter the curve, the more adequate the sequencing results are to reflect the diversity contained in the current samples [12], and the results in Fig. 3A and Fig.3B indicate that the sequencing depth of each sample is reasonable

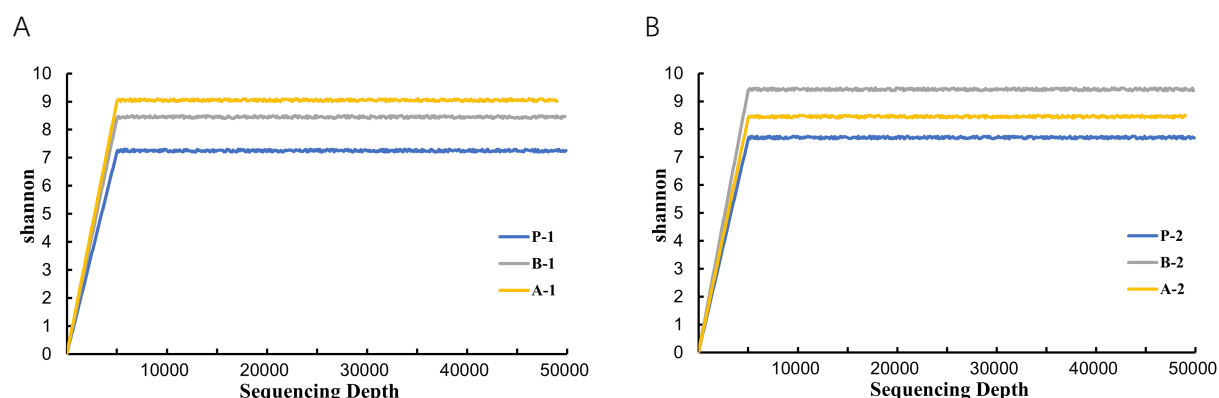


Fig. 3 Plot of sparse curves of Shannon index.

## 4. Differences in the composition and distribution of dominant genera

### 4.1 Compositional abundance of sample dominant genera

For 16S rRNA genes of bacteria or archaea, the Greengenes database [13] and the Silva database [14] were selected for this paper and species annotation was performed with the help of QIIME2 software. The distribution of the composition of each sample at the two taxonomic levels of the genus was analyzed by presenting the results in bar charts using the validated character sequences obtained in section 2.2. As shown in Fig. 4:

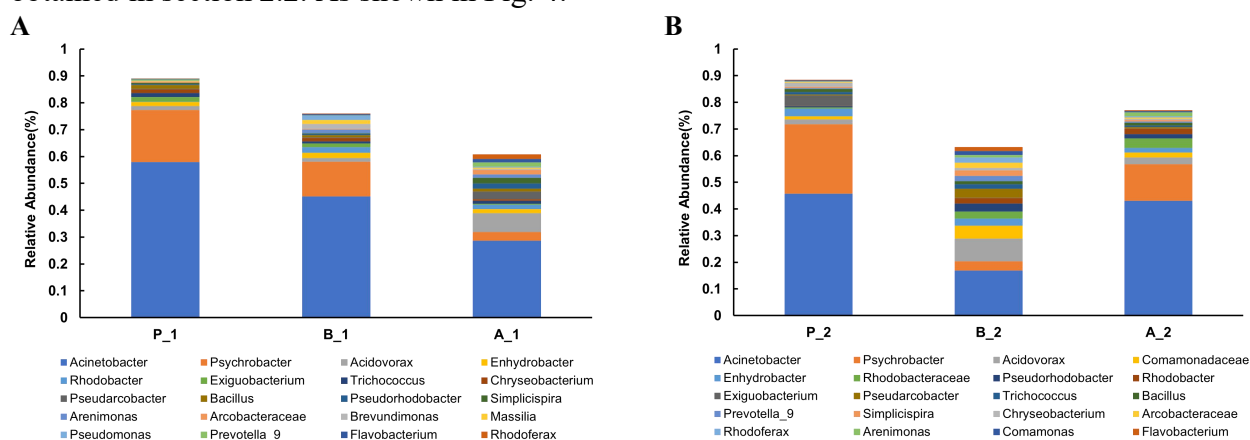


Fig. 4 Species distribution at genus level for different samples at different flow rates

As can be seen from the figure, Acinetobacter, Psychrobacter and Acidovorax were the dominant genera in the six samples. Among them, the compositional abundance of the dominant genera in the planktonic state was the highest, which could reach 70%~80% in the high/low flow rate environments; the compositional abundance of planktonic genera and benthic genera in the high flow rate area was larger than that in the low flow rate area, in which the difference in compositional abundance of benthic genera was about 30%; for the attached genera, the compositional abundance in the low flow rate area was larger than that in the high flow rate area by about 20%. This suggests that the dominant genera survive more in the planktonic state in the flowing waters; for the different flow velocity areas, the high flow velocity inhibited the dominant genera's attachment behavior on the surface of the structures and promoted their benthic behavior.

## 4.2 Differences in compositional abundance of dominant genera in mixed samples

To investigate which species are shared and which are unique among different samples (groups), we used the ASV/OUT numbers of each sample to plot a Wayne diagram for community analysis as shown in Fig. 5.

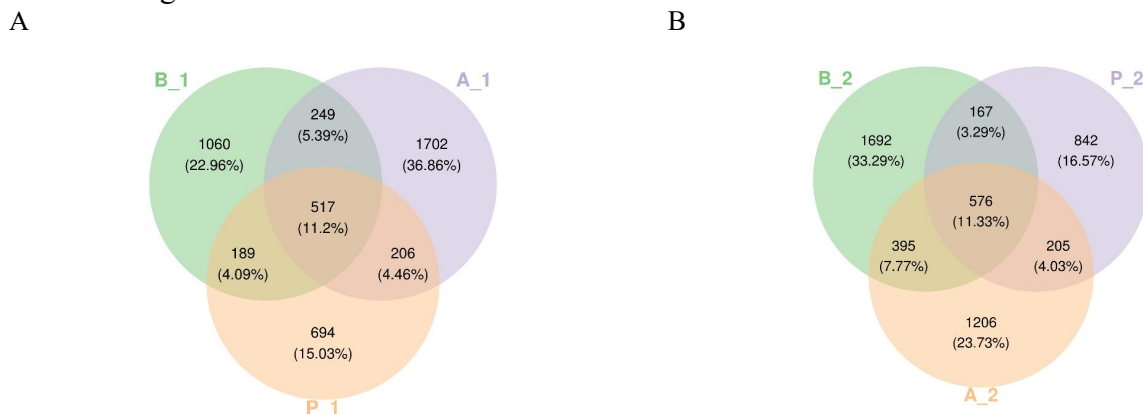


Fig. 5 Wayne diagram of sample (group) ASVs/OTUs.

In addition, the species abundance composition of each region in the Wayne diagram was further explored, i.e., the abundance of the corresponding ASVs/OTUs in each region was counted at the genus level and presented using bar charts.

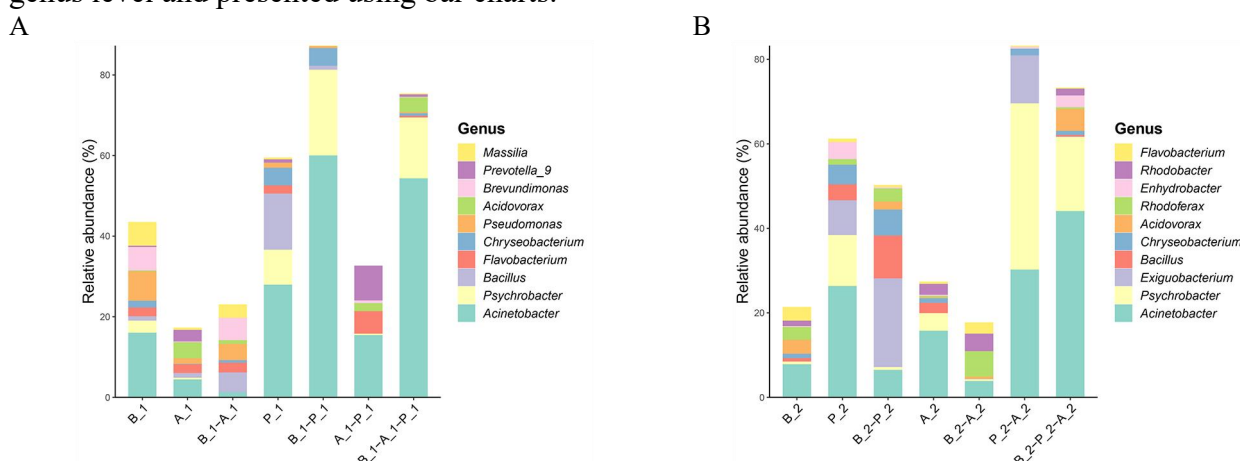


Fig. 6 Abundance maps of species composition for each region of the Wayne diagram.

The above results showed that *Acinetobacter* and *Psychrobacter* were the dominant genera in most of the single-sample or multi-sample overlap regions, with absolute abundance advantages. The analysis of species composition in the overlap samples showed that the species abundance in the P-A overlap region of the high-flow rate region was about 50% lower than that in the low-flow rate region. About 40% higher species abundance was found in the B-P overlap region of the high-flow zone than in the low-flow zone, suggesting that the flow rate altered the structure of species composition and the compositional abundance of dominant species in single-sample or multi-sample overlap regions.

## Conclusion

In this paper, samples collected from different flow velocity zones (0.794m/s and 0.538m/s) were identified and analyzed by high throughput demand measurement, and the results indicated that *Acinetobacter* and *Psychrobacter* were the dominant genera, and their compositional abundance in planktonic state could reach 70%~80%. In the high-flow zone, the compositional abundance of

benthic bacteria was about 30% higher than that in the low-flow zone, while the compositional abundance of adherent bacteria was about 20% lower than that in the low-flow zone. The above results indicated that the dominant genera survived more in the floating state in the flowing water body, and that the high flow rate inhibited the adherence of the dominant genera on the surfaces of the structures, and facilitated the benthic behavior of the dominant genera. Species composition analyses of the overlap samples showed that species abundance in the planktonic-attached overlap zone in the high-flow zone was about 50% lower than in the low-flow zone, and that species abundance in the benthic-planktonic overlap zone was about 40% higher than in the low-flow zone, suggesting that flow velocity altered the structure of the species composition of the multispecies overlap zone and the compositional abundance of dominant species. The conclusions drawn in this paper provide new perspectives for controlling microbial erosion and pollution in the waters of concern.

## Reference

- [1] Warscheid T, Braams J. Biodeterioration of stone: a review. *Int Biodeterior Biodegradation*, 2000, 46(4):343–68.
- [2] Videla HA, Herrera LK. Microbiologically influenced corrosion: looking to the future. *Int Microbiol*, 2005; 8(3):169.
- [3] Videla HA, Herrera LK. Understanding microbial inhibition of corrosion. A comprehensive overview. *Int Biodeterior Biodegradation*. 2009; 63(7):896–900.
- [4] Proco'pio L. The era of 'omics' technologies in the study of microbiologically influenced corrosion. *Biotechnol Lett*. 2020; 42(3):341–56.
- [5] Beech IB, Sunner JA, Hiraoka K. Microbe-surface interactions in biofouling and biocorrosion processes. *Int Microbiol*, 2005; 8(3):157–68.
- [6] Uehlinger, U. R. S., H. Bu'hrer & P. Reichert. Periphyton dynamics in a floodprone prealpine river: evaluation of significant processes by modelling. *Freshwater Biology*, 1996, 36:249–263.
- [7] P. Ramasamy, X. Zhang, Effects of shear stress on the secretion of extracellular polymeric substances in biofilms, *Water Sci. Technol*, 1996, 52 (7): 217–223.
- [8] I. Douterelo, R.L. Sharpe, S. Husband, K.E. Fish, J.B. Boxall, Understanding microbial ecology to improve management of drinking water distribution systems. *Wires Water*, 2019, 6 (1).
- [9] Kastl A, Bogler A, Spinnler M, et al. Impact of hydrodynamics on the first stages of biofilm formation in forward osmosis with spacers. *Environmental science & technology*, 2020, 54(8): 5279-5287.
- [10] Zhang J, Dong F, Liu S, et al. Biofilm streamer growth dynamics in various microfluidic channels. *Canadian Journal of Microbiology*, 2022, 68(5): 367-375.
- [11] Shannon CE. A mathematical theory of communication. *ACM SIGMOBILE mobile computing and communications review*. Nokia Bell Labs, 2001, 5(1):3-55.
- [12] Shannon P, Markiel, A, Ozier O, Baliga N S, Wang J T, Ramage D, Ideker T. Cytoscape: a software environment for integrated models of biomolecular interaction networks. *Genome Res*, 2003, 13(11):2498-2504.
- [13] DeSantis, T.Z., Hugenholtz, P., Larsen, N., Rojas, M., Brodie, E.L., Keller, K., Huber, T., Dalevi, D., Hu, P., and Andersen, G.L. (2006). Greengenes, a chimera-checked 16S rRNA gene database and workbench compatible with ARB. *Appl Environ Microbiol* 72, 5069-5072.
- [14] Quast, C., Pruesse, E., Yilmaz, P., Gerken, J., Schweer, T., Yarza, P., Peplies, J., and Gloeckner, F.O. (2013). The SILVA ribosomal RNA gene database project: improved data processing and web-based tools. *Nucleic Acids Res* 41, D590-D596.